Ground-state structure determination and mechanical properties of palladium seminitride*

Zhang Gang-Tai(张刚台)[a)†], Bai Ting-Ting(白婷婷)[b)], Zhao Ya-Ru(赵亚儒)[a)], and Lu Cheng(卢 成)[c)]

[a)] *Department of Physics and Information Technology, Baoji University of Arts and Sciences, Baoji* 721016, *China*
[b)] *Department of Mathematics, Baoji University of Arts and Sciences, Baoji* 721013, *China*
[c)] *Department of Physics, Nanyang Normal University, Nanyang* 473061, *China*

(Received 17 March 2013; revised manuscript received 13 May 2013)

Combining first-principles calculations with the particle swarm optimization (PSO) algorithm, we have explored the ground-state structure of Pd_2N, whose structure is in debate although it is the first synthesized binary platinum group nitride. The ground-state structure is predicted to be tetragonal with space group $P\bar{4}m2$, which is energetically more favorable than the previously proposed orthorhombic Co_2N-type structure. The stability is confirmed by the subsequent calculations on the phonon dispersion curves and elastic constants. Furthermore, the calculated mechanical properties indicate that Pd_2N has low incompressibility and is a common hard material.

Keywords: Pd_2N, particle swarm optimization algorithm, ground-state structure, first-principles calculations

PACS: 61.66.Fn, 61.50.Ah, 62.20.de **DOI:** 10.1088/1674-1056/22/11/116104

1. Introduction

One of the great challenges in theoretical material science is the development of a robust method that can predict the (meta)stable structure of a chemical system. For systems in which the cohesion of the atomic arrangement is dominated by chemical bonding, such as ionic or covalent systems, simple atom-interaction models can be combined with the experimental evidence to generate reasonable structural candidates with a relatively small amount of effort.[1,2] Transition metal nitrides are of great technological and fundamental importance due to excellent properties such as hardness, superconductivity, photoluminescence, and many types of magnetism.[3–6] The traditional applications have taken advantage of the hard and refractory nature of many of these compounds, but numerous more recent applications are based on their crystalline structure stability, mechanical, electronic, optical, and vibrational properties. Following the recently synthesized ultra-incompressible platinum nitride (PtN_2),[7] the nitrides of Ir, Os, Pd, and Re with high nitrogen/metal ratios were successfully synthesized under high pressure and high temperature.[8–11] Except for PdN_2, all those compounds have been shown to be at least metastable at ambient conditions and possess ultra-high bulk moduli (428 GPa for IrN_2). Extensive experimental and theoretical works have been carried out to characterize the preference of the structure types of different stoichiometric transition metal nitrides. Experimentally, Friedrich *et al.*[12] have succeeded in synthesizing two novel hexagonal rhenium nitrides with low nitrogen contents (Re_3N and Re_2N), and both hexagonal phases have very high bulk moduli (> 400 GPa), which are comparable to that of *c*-BN and higher than that of ReB_2. Theoretically, the structural stability and related physical properties of low-nitrogen compounds Co_2N, Rh_2N, and Ir_2N[13] were investigated by density functional methods.

It is well known that the crystal structures are the key for understanding the physical properties of materials. Compared to the transition metal nitrides mentioned above, the ground-state structure of Pd_2N, which is the first synthesized binary platinum group nitride, is still the subject of continuing debate. Pd_2N was first detected as a 2.29% by-product in the X-ray powder diffraction pattern of Pd_2Mo_3N by Prior and Battle in 2003.[14] According to that report, Pd_2N was suggested to possess an orthorhombic Co_2N-type structure (*Pmnn*, $Z = 2$). In 2004, that Co_2N-type structure was made part of the International Crystal Structure Database (ICSD).[15] Later, Appen and Dronskowski[16] found that Pd_2N of Co_2N type fully collapses and changes to a tetragonal unit cell by re-calculation optimizing the experimental structural parameters, and proposed that Pd_2N should crystallize in a tetragonal structure. However, the detail crystal parameters including internal atomic positions of the suggested tetragonal structure are still unknown. To the best of our knowledge, there has been no attempt to synthesize single-phase Pd_2N. Therefore, the exploration of the ground-state structure of Pd_2N is still required. In our present work, we have systematically explored the ground-state structure of Pd_2N based on a global minimization of free-energy surfaces merging *ab initio* total energy calculations via the particle swarm optimization (PSO) technique.[17,18] Intriguingly, our structural prediction reveals a stable tetragonal $P\bar{4}m2$ structure, which is energetically more favorable than the

*Project supported by the Science Foundation of Baoji University of Arts and Sciences, China (Grants Nos. ZK11061, ZK11135, and ZK12048), the Natural Science Foundation of the Education Committee of Shaanxi Province, China (Grant Nos. 2013JK0637 and 2013JK0638), and the Natural Science Basic Research Plan in Shaanxi Province, China (Grant No. 2013JQ1007).

†Corresponding author. E-mail: gtzhang79@163.com

© 2013 Chinese Physical Society and IOP Publishing Ltd

previously proposed Co_2N-type structure. Then, the structural intrinsic connections between pure Pd metal and $P\bar{4}m2$-Pd_2N are studied to investigate the incorporation of N into the Pd lattice. Moreover, we investigate the mechanical and electronic properties. These theoretical calculations can provide further details and are highly desirable.

2. Computational details

The PSO methodology for crystal structural prediction has been implemented in the crystal structure analysis by particle swarm optimization (CALYPSO) code[19] with 1–4 formula units (f.u.) per simulation cell. The details of this methodology have been described elsewhere.[18] The underlying *ab initio* calculations were carried out using density functional theory within the generalized gradient approximation, as implemented in the Vienna *ab initio* simulation package (VASP).[20] The electron and core interactions were included by using the frozen-core all-electron projector augmented wave method,[21] which considered the d electrons as the valence states for Pd. To reduce the errors, the cut-off energy for the expansion of the wave function into plane waves was set to 450 eV in all calculations, and the Monkhorst–Pack grid[22] had a maximum spacing of 0.03 $Å^{-1}$. In the geometrical optimization calculations, all forces were converged to less than 0.001 eV/Å. The total stress tensor was reduced to be within 0.01 GPa. The phonon frequency was calculated by using the direct approach, which based on the first-principles calculations of the Hellman–Feynman forces and the dynamical matrix as implemented in the PHONOPY code.[23] The elastic constants were calculated by evaluating the stress tensor to generate a small strain. The bulk modulus, the shear modulus, Young's modulus, and Poisson's ratio were derived from the Voigt–Reuss–Hill approximation.[24]

3. Results and discussion

Considering the simulation cell ranging from one f.u. to four f.u. for Pd_2N, we predict the most stable structure to be the tetragonal $P\bar{4}m2$ structure, as shown in Fig. 1(b). This $P\bar{4}m2$ structure contains two f.u. per cell, in which three inequivalent atoms N, Pd1, and Pd2 occupy the Wyckoff 2*f* (0.5, 0.5, 0.058), 2*g* (0, 0, 0.406), and 2*g* (0, 0, 0.788) sites, respectively. As observed in Fig. 1(b), this $P\bar{4}m2$ structure is characterized by intriguing Pd–N–Pd sandwiches stacking along the crystallographic *c* axis. The N–N bond distance in the predicted Pd_2N is 1.17 Å, much shorter than $\sim$ 1.4 Å observed in OsN_2[9] and PtN_2,[8] indicating the presence of more free-like N_2 quasimolecules. It is also noted that the short N–N bond distance of Pd_2N is close to the double-bond distance (1.21 Å for N_2F_2[25]), but much larger that the triple-bond distance (1.07 Å for molecular nitrogen[26]), implying its possible double-bond feature. For the cubic 2×2×2 supercell Pd presented in Fig. 1(a), the cubic Pd phase consists of a body-centered tetragonal sublattice (blue dashed cell) with lattice constants $a = b = 2.751$ Å and $c = 3.891$ Å along the *c* axis. If we consider a 2×1×1 supercell for tetragonal $P\bar{4}m2$ phase in Fig. 1(b), we can see that this $P\bar{4}m2$-Pd_2N consists of two different fundamental building blocks along the *c* axis: tetragonal Pd sublattice I (blue dashed cell with lattice constants $a = b = 2.875$ Å and $c = 3.857$ Å) and tetragonal Pd sublattice II including N_2 quasimolecules (red dashed cell with lattice constants $a = b = 2.875$ Å and $c = 6.250$ Å). In this approach, the interaction of the N atoms into the Pd lattice for the formation of $P\bar{4}m2$-Pd_2N could be understood as follows. The N atoms incorporate into the Pd body-centered tetragonal sublattice with an interval (which would be possible from the packing considerations), this leads to the formation of two building blocks for $P\bar{4}m2$-Pd_2N: tetragonal sublattices I and II.

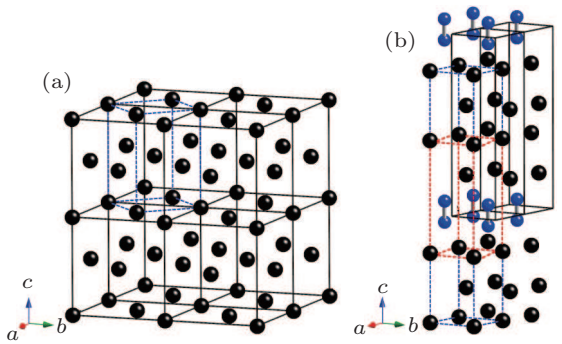


Fig. 1. (color online) Crystal structures of (a) pure 2×2×2 Pd metal and (b) 2×1×1 supercell of $P\bar{4}m2$-Pd_2N. The black and blue spheres represent Pd and N atoms, respectively.

To calculate the equilibrium lattice constants and bulk modulus, the total energy is calculated by varying the volume for $P\bar{4}m2$-Pd_2N. The calculated *E*–*V* data are fitted to the third-order Birch–Murnaghan equation of state,[27] and the obtained equilibrium structure parameters, bulk modulus, and its pressure derivative are tabulated in Table 1 together with the experimental data of Co_2N-Pd_2N[14,15] for comparison. Figure 2 presents the dependences of the total energy on the volume for $P\bar{4}m2$-Pd_2N and Co_2N-Pd_2N. It is clearly that the $P\bar{4}m2$ phase is energetically far more stable than the Co_2N phase, and this further confirms our structural prediction. At zero temperature, a stable crystalline structure requires all phonon frequencies to be positive. Therefore, we perform the phonon dispersion calculation for Co_2N-Pd_2N and $P\bar{4}m2$-Pd_2N, as shown in Fig. 3. For Co_2N-Pd_2N shown in Fig. 3(a), it is clearly seen that the phonon spectrum shows a large imaginary frequency, signaling its structural instability. However, no imaginary phonon frequency is found in the whole Brillouin zone for $P\bar{4}m2$-Pd_2N in Fig. 3(b), supporting its dynamical stability. Therefore, the present calculation gives a direct evidence that the predicted tetragonal $P\bar{4}m2$ structure for Pd_2N is indeed the ground-state structure.

Table 1. Calculated equilibrium lattice constants a_0, b_0, c_0, equilibrium volume V_0, EOS fitted bulk modulus B_0, and its pressure derivative B_0' for $P\bar{4}m2$-Pd_2N and Co_2N-Pd_2N.

	a_0/Å	b_0/Å	c_0/Å	V_0/(Å^3/unit cell)	B_0/GPa	B_0'
$P\bar{4}m2$-Pd_2N	2.875	2.875	10.107	83.552	120	6.107
Co_2N-Pd_2N	2.808[14]	4.863[14]	4.487[14]	61.270[15]	158	5.576

Table 2. Calculated elastic constants C_{ij} (in units of GPa), isotropic bulk modulus B_H, shear modulus G_H, and Young's modulus E_H for $P\bar{4}m2$-Pd_2N. Poisson's ratio ν_H and B_H/G_H ratio are also shown.

	C_{11}	C_{22}	C_{33}	C_{44}	C_{55}	C_{66}	C_{12}	C_{13}	C_{23}	B_H/GPa	G_H/GPa	B_H/G_H	E_H/GPa	ν_H
$P\bar{4}m2$-Pd_2N	181	–	213	62	–	16	73	122	–	145	40	3.625	111	0.372
Co_2N-Pd_2N	202	236	185	67	47	39	126	140	155	185	42	4.405	117	0.394
Co_2N-Rh_2N[13]	371	293	351	88	36	122	248	215	187	254	66	3.85	–	–
Co_2N-Ir_2N[13]	479	390	509	174	56	197	279	261	270	331	111	2.98	–	–

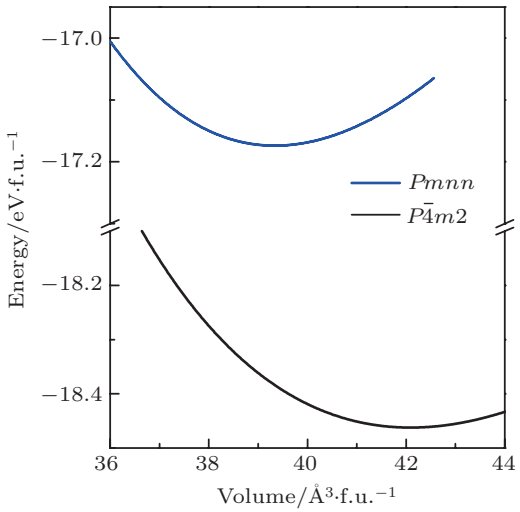


Fig. 2. (color online) Total energy versus volume for $P\bar{4}m2$-Pd_2N and Co_2N-Pd_2N.

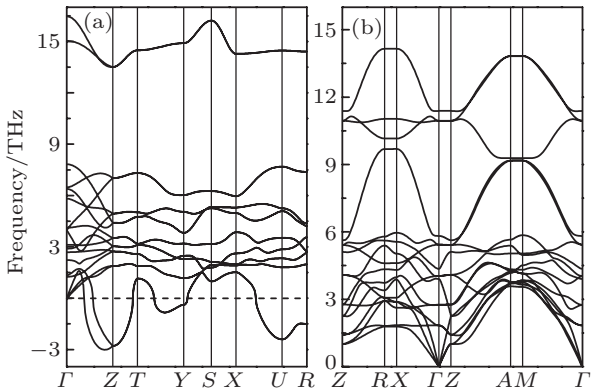


Fig. 3. Phonon dispersion curves of (a) Co_2N-Pd_2N and (b) $P\bar{4}m2$-Pd_2N.

The mechanical properties of $P\bar{4}m2$-Pd_2N are important for its potential technological and industrial applications. They define the behavior of the solid that undergoes stress, deforms, then recovers, and returns to its original shape after the stress ceases. We calculate the zero-pressure elastic constants C_{ij} of the $P\bar{4}m2$ phase by the strain-stress method.[28] A small finite strain is applied on the optimized structure and the atomic positions are fully optimized. Then, the elastic constants are obtained from the stress of the strained structure. The six independent zero pressure elastic constants are calculated and listed in Table 2, along with the theoretical values of Pd_2N, Rh_2N, and Ir_2N within Co_2N-type structure[13] for comparison. A tetragonal crystal has to obey the following restrictions on its elastic constants:[29] $C_{11} > 0$, $C_{33} > 0$, $C_{44} > 0$, $C_{66} > 0$, $C_{11} - C_{12} > 0$, $C_{11} + C_{33} - 2C_{13} > 0$, $2(C_{11} + C_{12}) + C_{33} + 4C_{13} > 0$. As shown in Table 2, these restrictions are clearly satisfied for tetragonal stability, confirming that $P\bar{4}m2$-Pd_2N is mechanically stable. It is interesting to find that the elastic constant C_{44} of $P\bar{4}m2$-Pd_2N, which relates to the shear modulus within the (001) plane,[30] is only 62 GPa. It means that the $P\bar{4}m2$ phase can be easily cleavaged with an applied (001) shear deformation, originated from the pure weak Pd–Pd metallic bonding layers in Fig. 1(b). Using the obtained elastic constants, the bulk modulus B_H and shear modulus G_H are evaluated by using the Voigt–Reuss–Hill approximation, as shown in Table 2. The Young's modulus E_H and Poisson's ratio ν_H are derived from the equations $E_H = 9B_HG_H/(3B_H + G_H)$ and $\nu_H = (3B_H - 2G_H)/(6B_H + 2G_H)$. It should be noted that the calculated bulk moduli of $P\bar{4}m2$-Pd_2N and Co_2N-Pd_2N agree with those directly obtained from the fitting of the third-order Birch–Murnaghan equation of state, this further demonstrates the reliability of our elastic calculations. Compared to Co_2N-Rh_2N and Co_2N-Ir_2N, $P\bar{4}m2$-Pd_2N has a smaller bulk modulus (145 GPa), indicating a low-incompressible nature. For the partially covalent transition metal based hard materials, the shear modulus has been considered as a very important parameter, governing the indentation hardness. Clearly, the G_H of $P\bar{4}m2$-Pd_2N is 40 GPa, which is much lower than that of synthesized platinum group dinitrides.[7–11] Thus, $P\bar{4}m2$-Pd_2N is expected to withstand the shear strain to a small extent. Here, the estimated theoretical Vickers hardness for $P\bar{4}m2$-Pd_2N using the empirical G–H_v and E–H_v relationships proposed by Jiang *et al.*[31,32] is 5.9–6.7 GPa. In addition, the ratio between the bulk and the shear

moduli B/G is used to predict the brittle or ductile behavior of materials. According to the Pugh criterion,[33] the ductile behavior is predicted when $B/G > 1.75$, otherwise the material would be brittle. It can be clearly seen in Table 2 that $P\bar{4}m2$-Pd_2N is strongly prone to the ductile manner.

As a fundamental parameter, the Debye temperature closely relates to many physical properties of solids, such as the specific heat, dynamic properties, and melting temperature.[34] At low temperature, it can be derived from the elastic constants using the average sound velocity v_m by the following equation:

$$\Theta_D = \frac{h}{k}\left[\frac{3n}{4\pi}\left(\frac{\rho N_A}{M}\right)\right]^{1/3} v_m, \quad (1)$$

where h is Planck's constant, k is Boltzmann's constant, N_A is Avogadro's number, n is the number of atoms per formula unit, M is the molecular mass per f.u., and ρ is the density. The average sound velocity v_m is given by

$$v_m = \left[\frac{1}{3}\left(\frac{2}{v_t^3} + \frac{1}{v_l^3}\right)\right]^{-1/3}, \quad (2)$$

where v_t and v_l are the transverse and longitudinal elastic wave velocities of the polycrystalline material and are given by Navier's equation.[35] The results indicate that the Debye temperature of $P\bar{4}m2$-Pd_2N is only 294 K, which may be attributed to the lower shear modulus.

To understand the mechanical properties of the $P\bar{4}m2$ phase on the fundamental level, the total and partial densities of states (DOS) are calculated and plotted in Fig. 4, where the vertical line is the Fermi level. From the total DOS, we find that $P\bar{4}m2$-Pd_2N exhibits a clear metallic behavior as evidenced by the finite electronic DOS at the Fermi level, indicating good electronic mobility in Pd_2N. This is similar to many other transition metal nitrides.[7–11,36] The typical feature of the total DOS is the presence of the so-called pseudogap,[37] which is considered as the borderline between the bonding and antibonding states. It can be seen that the calculated Fermi energy is located below the pseudogap for $P\bar{4}m2$-Pd_2N, indicating that its bonding states are partially occupied and full antibonding states are unoccupied. As can be seen from partial DOS of Pd_2N in Fig. 4, the lowest band, which lies about 11 eV below the Fermi level, can be attributed to the N 2s states. Above the band, there is a many-band complex, which has a width of approximately 9 eV and N 2p and Pd 4d character. Meanwhile, it reveals that the Pd-4d orbital has a significant hybridization with the N-2p orbital, indicating the strong Pd–N covalent bonding nature within the sandwich layers. The contribution to the Fermi level is mainly due to the 4d electrons of Pd, which is the principal cause for the metallicity. It is not surprise that $P\bar{4}m2$-Pd_2N reveals a metallic behavior, as it contains Pd atom chains along the [001] crystal direction with an average Pd–Pd distance of 2.803 Å compared to the value of 2.751 Å in cubic Pd.

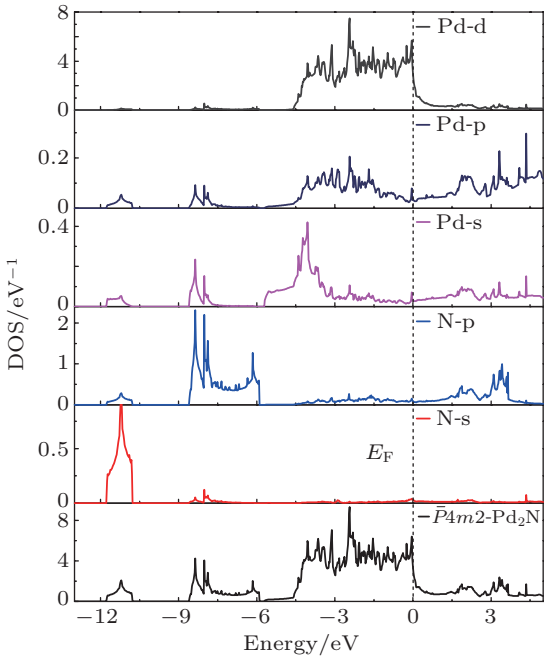


Fig. 4. (color online) Total and partial densities of states of $P\bar{4}m2$-Pd_2N.

4. Conclusion

In summary, we have predicted that Pd_2N energetically favors the tetragonal $P\bar{4}m2$ structure at ground state through PSO algorithm for crystal structural predictions. The structural, mechanical, and electronic properties of $P\bar{4}m2$-Pd_2N have been investigated by first-principles calculations. The total energy calculations reveal that the predicted tetragonal $P\bar{4}m2$ structure is energetically more stable than the previous reported Co_2N-type structure. The stability is confirmed by the elastic constants and phonon calculations. The calculated bulk modulus, shear modulus, and hardness of the $P\bar{4}m2$ phase are much smaller than those of synthesized platinum group dinitrides. Hence, our results support that $P\bar{4}m2$-Pd_2N has low incompressibility, and it is a common hard material, but not a candidate superhard material. The electronic density of states analysis has unraveled the good metallicity of $P\bar{4}m2$-Pd_2N and the covalent bonding between Pd and N atoms.

References

[1] Cohen M L 1989 *Nature* **338** 291
[2] Woodley S M and Catlow C R A 2008 *Nat. Mater.* **7** 937
[3] Kaner R B, Gilman J J and Tolbert S H 2005 *Science* **308** 1268
[4] Chung H Y, Weinberger M B, Levine J B, Kavner A, Yang J M, Tolbert S H and Kaner R B 2007 *Science* **316** 436
[5] Zerr A, Riedel R, Sekine T, Lowther J E, Ching W Y and Tanaka I 2006 *Adv. Mater.* **18** 2933
[6] Horvath-Bordon E, Riedel R, Zerr A, McMillan P F, Auffermann G, Prots Y, Bronger W, Kniep R and Kroll P 2006 *Chem. Soc. Rev.* **35** 987
[7] Crowhurst J C, Goncharov A F, Sadigh B, Evans C L, Morrall P G, Ferreira J L and Nelson A J 2006 *Science* **311** 1275
[8] Young A F, Sanloup C, Gregoryanz E, Scandolo S, Hemley R J and Mao H K 2006 *Phys. Rev. Lett.* **96** 155501

[9] Gregoryanz E, Sanloup C, Somayazulu M, Badro J, Fiquet G, Mao H K and Hemley R J 2004 *Nat. Mater.* **3** 294
[10] Crowhurst J C, Goncharov A F, Sadigh B, Zaug J M, Aberg D, Meng Y and Prakapenka V B 2008 *J. Mater. Res.* **23** 1
[11] Kawamura F, Yusa H and Taniguchi T 2012 *Appl. Phys. Lett.* **100** 251910
[12] Friedrich A, Winkler B, Bayarjargal L, MorgenrothW, Juarez-Arellano E A, Milman V, Refson K, Kunz M and Chen K 2010 *Phys. Rev. Lett.* **105** 085504
[13] Wu Z and Zhao E 2008 *J. Phys. Chem. Solids* **69** 2723
[14] Prior T J and Battle P D 2003 *J. Solid State Chem.* **172** 138
[15] ICSD, FIZ Karlsruhe, #96418, 2004/04/01
[16] Appen J V and Dronskowski R 2006 *Z. Anorg. Allg. Chem.* **632** 2105
[17] Wang Y C, Lv J, Zhu L and Ma Y M 2010 *Phys. Rev. B* **82** 094116
[18] Wang Y C, Lv J, Zhu L and Ma Y M 2012 *Comput. Phys. Commun.* **183** 2063
[19] Ma Y M, Wang Y C, Lv J and Zhu L http://www.calypso.cn/
[20] Kresse G and Furthmüller J 1996 *Phys. Rev. B* **54** 11169
[21] Kresse G and Joubert D 1999 *Phys. Rev. B* **59** 1758
[22] Monkhorst H J and Pack J D 1976 *Phys. Rev. B* **13** 5188
[23] Togo A, Oba F and Tanaka I 2008 *Phys. Rev. B* **78** 134106
[24] Hill R 1952 *Proc. Phys. Soc. A* **65** 349
[25] Herndon W C, Feuer J and Hall L H 1968 *Theor. Chim. Acta* **11** 178
[26] Stoicheff B P 1954 *Can. J. Phys.* **32** 630
[27] Birch F 1947 *Phys. Rev.* **71** 809
[28] Zhao W J, Xu H B and Wang Y X 2010 *Chin. Phys. B* **19** 016201
[29] Born M 1940 *Proc. Cambridge Philos. Soc.* **36** 160
[30] Zhang M G, Yan H Y, Wei Q and Wang H 2012 *J. Appl. Phys.* **112** 013522
[31] Jiang X, Zhao J J and Jiang X 2011 *Comp. Mater. Sci.* **50** 2287
[32] Zhang M G, Yan H Y, Zhang G T and Wang H 2012 *Chin. Phys. B* **21** 076103
[33] Pugh S F 1954 *Philos. Mag.* **45** 823
[34] Ravindran P, Fast L, Korzhavyi P A, Johansson B, Wills J and Eriksson O 1998 *J. Appl. Phys.* **84** 4891
[35] Anderson O L 1963 *J. Phys. Chem. Solids* **24** 909
[36] Li C B, Li M K, Yin D, Liu F Q and Fan X J 2005 *Chin. Phys.* **14** 2287
[37] Vajeeston P, Ravindran P, Ravi C and Asokamani R 2001 *Phys. Rev. B* **63** 045115